Ab initio Calculations of Deep-Level Carrier Nonradiative Recombination Rates in Bulk Semiconductors

Lin Shi[1,2] and Lin-Wang Wang[1,*]

[1]*Materials Sciences Division, Lawrence Berkeley National Laboratory, One Cyclotron Road, Mail Stop 66, Berkeley, California 94720, USA*

[2]*Suzhou Institute of Nano-Tech and Nano-Bionics, Chinese Academy of Sciences, Suzhou 215125, People's Republic of China*

(Received 8 June 2012; published 10 December 2012)

Nonradiative carrier recombination is of both applied and fundamental interest. Here a novel algorithm is introduced to calculate such a deep level nonradiative recombination rate using the *ab initio* density functional theory. This algorithm can calculate the electron-phonon coupling constants all at once. An approximation is presented to calculate the phonon modes for one impurity in a large supercell. The neutral Zn impurity site together with a N vacancy is considered as the carrier-capturing deep impurity level in bulk GaN. Its capture coefficient is calculated as 5.57×10^{-10} cm^3/s at 300 K. We found that there is no apparent onset of such a nonradiative process as a function of temperature.

DOI: 10.1103/PhysRevLett.109.245501 PACS numbers: 63.20.dk, 61.72.S−, 72.10.Di

Nonradiative carrier recombination as often described by the Shockley-Read-Hall (SRH) [1–3] model is a very important process in semiconductor physics. Unfortunately, direct measurement of such processes is scarce [4–9], and reliable data are not always available. Unfortunately, since the early analytical work of the 1950s and 1960s [10–13], there is a lack of progress in terms of *ab initio* calculation in this field. On the other hand the nonradiative decay processes have been calculated in quantum chemistry for molecules [14–16], and the fundamental formalism describing the multiphonon process was well established long ago [13] and has been proved to be quantitatively accurate for molecular systems [14–16]. One challenge to apply such formalism to bulk semiconductor impurity is the large computational cost, which prevents the application of the *ab initio* calculations to these problems. Here, we introduce a new algorithm, which calculates the electron-phonon coupling constants all at once, and makes it possible to use *ab initio* density functional theory (DFT) to calculate the deep level nonradiative decay rate in a semiconductor. This new method can also be used to study other multiphonon emission related charge transports, e.g., carrier cooling, interface transport, surface state trapping, and quantum dot charge transfer [17,18].

GaN has attracted great interest over the past two decades as a material for blue and ultraviolet light-emitting devices [19,20]. Synthesized GaN often contains unintentionally doped Zn impurity accompanying a characteristic blue shift in photoluminescence (PL) [5–8], and also a sharp drop in PL intensity, due to nonradiative decay. Although the exact nature of the nonradiative decay center is still under debate, it is suggested [5] that it could be $Zn_{Ga}V_N$, a Zn impurity site together with a N vacancy as shown in the inset of Fig. 1. The experimentally fitted nonradiative capture rate ranges from 3×10^{-6} cm^3/s to 3×10^{-10} cm^3/s [5–9], highlighting the importance of using an *ab initio* method to clarify the situation.

A 299-atom ($5 \times 5 \times 3$) supercell is used to calculate the formation energy of the $Zn_{Ga}V_N$ center following the procedure of Refs. [21–24] using the screened hybrid functional of Heyd, Scuseria, and Ernzerhof (HSE) [25,26] and generalized gradient approximation (GGA) atomic relaxation. The cutoff for the plane-wave basis is 400 eV. The mixing parameter of HSE was set to 0.25 [25,26]. The GGA calculated equilibrium lattice parameters of GaN, $a = 3.20$ Å, $c = 5.22$ Å, and $u = 0.377$, agree well with experimental results ($a = 3.20$ Å, $c = 5.22$ Å, and $u = 0.377$) [27]. This part of the calculation uses the

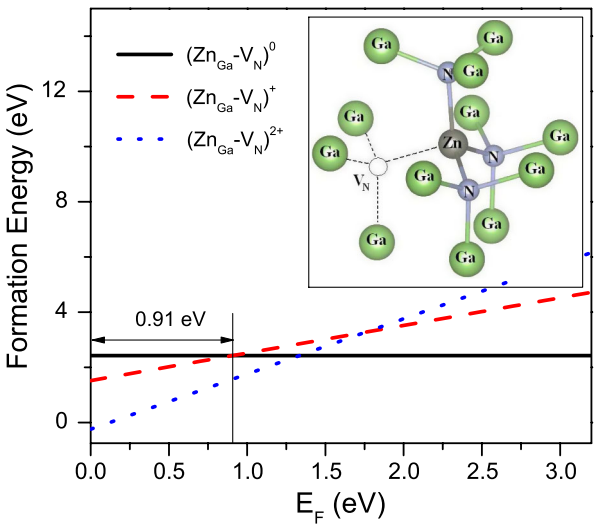

FIG. 1 (color online). The formation energy of $Zn_{Ga}V_N$ at different charge states calculated under HSE, and the atom structure for the $Zn_{Ga}V_N^+$ is shown in the inset. E_F is the electron Fermi energy. E_F zero is defined at the valence band maximum.

commercial code VASP (the Vienna *ab initio* simulation package) [28]. Following Ref. [29], the formation energy ΔE^q of the $Zn_{Ga}V_N$ defect with charge q is calculated as

$$\Delta E^q = E^q_{sc} - E_{bulk}(GaN) - \mu(Zn) + \mu(Ga) + \mu(N) + q[E_F + \epsilon_{VBM}(host)], \quad (1)$$

with the chemical potentials $\mu(Zn)$, $\mu(Ga)$ calculated from their metallic states and $\mu(N)$ taken from the N poor condition [$\mu(N) = E^{percell}_{bulk}(GaN) - \mu(Ga)$]. E_F is the Fermi energy, with zero defined at the bulk valence band maximum (VBM) energy ϵ_{VBM}. The calculated ΔE^q are shown in Fig. 1. Note, since the GaN in the experiment is *n* type, the $Zn_{Ga}V_N$ center should be at its neutral state. Comparing ΔE^0 with the separated Zn_{Ga} and V_N formation energies, we get the donor-acceptor binding energy as -0.79 eV. As a result, if there are N vacancies and Zn impurities, they will always form $Zn_{Ga}V_N$ donor-acceptor pairs. As shown in Fig. 1, the $2+/+$ transition energy is higher than the $+/0$ transition energy, forming a negative-U center, which is similar with $Mg_{Ga}V_N$ center [30].

As discussed above, the $Zn_{Ga}V_N$ center is neutral in an *n*-type GaN with its electronic states fully occupied. For it to be a nonradiative decay center, it will first accept a hole becoming +charged. This +charged center will be quickly neutralized by the majority electrons in the conduction band. Thus, the bottleneck, and the rate of the nonradiative decay will be determined from the hole to $Zn_{Ga}V_N$ process. Our HSE calculated transition energy for this process is 0.91 eV as shown in Fig. 1. The relevant electron-phonon coupling should be between the impurity states and the valence band states, which can be represented by the VBM state. The impurity state wave function is illustrated in Fig. 2 in a 299-atom supercell.

There are different theoretical treatments for the multiphonon assisted electronic transitions. In particular, there are adiabatic approximation treatments [10,31,32], and static coupling theory treatments [13,33]. As pointed out by Huang [34], these two approaches can be unified. In the current work, we will adopt the formula derived by Freed and Jortner [13] based on the static coupling approach using techniques similar to that of Lin [11]. Their formula is originally derived for large molecules for semicontinuous phonon density of states (DOS). It should be perfectly applicable to bulk systems like ours. We will use the strong coupling limit formula, with its justification given in the Supplemental Material [35]. In this formula, the electron transition rate between electron states s and l can be expressed as

$$W_{sl} = \sum_k \frac{|C^k_{sl}|^2 \omega_k (2\pi)^{1/2}}{2\hbar D}\Big[(\coth y_k + 1) \times \exp\Big(-\frac{(\Delta E_{sl} - \hbar\omega_k - E_M)^2}{2D^2\hbar^2}\Big) + (\coth y_k - 1) \times \exp\Big(-\frac{(\Delta E_{sl} + \hbar\omega_k - E_M)^2}{2D^2\hbar^2}\Big)\Big], \quad (2)$$

where k is the index of phonon mode with frequency ω_k, and $D^2 = \frac{1}{2}\sum_j \omega_j^2 \Delta_j^2 (2\bar{n}_j + 1)$, $\bar{n}_j = [\exp(\beta\hbar\omega_j) - 1]^{-1}$, $\Delta_j = (\frac{M_j\omega_j}{\hbar})^{1/2}(Q_j^{0(s)} - Q_j^{0(l)})$, and $y_k = \beta\hbar\omega_k/2$, $\beta = \frac{1}{kT}$. Here $Q_j^{0(s)}$ and $Q_j^{0(l)}$ are the relaxed ground state coordinations of phonon mode j at electron states s and l, which can be calculated as $Q_j^{0(s,l)} = \frac{1}{\sqrt{M_j}}\sum_R M_R \mu_j(R) R^{0(s,l)}$, here $R^{0(s,l)}$ are the relaxed atomic positions at electron states s and l, and $\mu_j(R)$ is the jth phonon mode [see Eq. (4)] with a normalization of $\sum_R M_R \mu_k(R)\mu_j(R) = \delta_{k,j}$, M_R is the atom mass (here R is used to denote the atom). M_j is the phonon mass, which can be arbitrarily defined without affecting the final result. $E_M = \frac{1}{2}\sum_j \hbar\omega_j \Delta_j^2$ is the reorganization energy (atomic relaxation energy after electron state transition). The ΔE_{sl} equals the total energy change between the atomic relaxed l and s electron states, hence 0.91 eV in our case (Fig. 1). C^k_{sl} is the coupling constant between electronic states s and l, and the phonon mode k, which will be discussed later.

Equation (2) implies that only a single mode phonon (promoting mode) and a single phonon of that mode is responsible for inducing the s to l transition in a given term of the $\sum_k$ sum, while the role of all the other phonon modes "j" (accepting modes) is to create or annihilate phonons due to $Q_j^{0(s)} - Q_j^{0(l)} \neq 0$ to satisfy the energy conservation law. For a given phonon mode, it can be the promoting mode in one term of $\sum_k$, while being the accepting mode in other terms. The electron phonon coupling constant in Eq. (2) between electronic states s and l and phonon mode k is

$$C^k_{sl} = \frac{i\hbar \sum_R \mu_k(R)\langle\psi_s|(\partial H/\partial R)|\psi_l\rangle}{\Delta E_{sl}}. \quad (3)$$

The connection of this formula to the original formula in Ref. [13] is given in the Supplemental Material [35]. In order to use Eqs. (2) and (3), we need to calculate: (a) the phonon mode $\mu_k(R)$ and its frequency ω_k and (b) the coupling constants $\langle\psi_s|(\partial H/\partial R)|\psi_l\rangle$. The reorganization energy

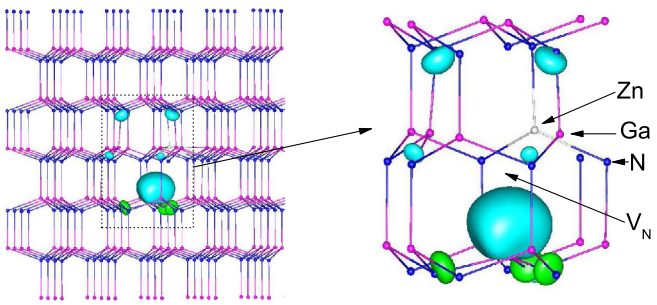

FIG. 2 (color online). The impurity wave function ψ_{im} of $Zn_{Ga}V_N^+$ in the 299-atom supercell calculated using the HSE DFT functional. The cyan (the biggest one and above 4) is a positive isosurface of the impurity wave function while the green (the 3 under the biggest one) is a negative isosurface.

E_M can be obtained directly by first calculating the neutral impurity $Zn_{Ga}V_N$ and its relaxed atomic coordinates $R_l^{(0)}$, then relax from this atomic configuration to get the $+$state atomic configuration $R_s^{(0)}$ and record the energy drop (E_M). Our HSE calculated E_M is 0.43 eV. In the following, we will use novel methods to calculate both quantities (a) and (b) above.

To get the phonon spectrum, we can diagonalize the dynamic matrix:

$$M(R_1, R_2) = \frac{1}{(M_{R_1} M_{R_2})^{1/2}} \frac{\partial^2 E}{\partial R_1 \partial R_2}. \quad (4)$$

The kth eigenvector of M will be $M_R^{1/2}\ \mu_k(R)$, and the eigenvalue will be $(\hbar\omega_k)^2$. Note $\partial^2 E/\partial R_1 \partial R_2 = \partial F_{R_1}(R_2)/\partial R_2$, thus we can numerically displace atoms R_2, while using the Hellman-Feynman theory to calculate the atomic forces $F_{R_1}(R_2)$ for all the atoms R_1. However, for a 299-atom supercell as we have above, this means $299 \times 3 = 897$ self-consistent field (SCF) DFT calculations.

Here we will use an approximation to get $\partial^2 E/\partial R_1 \partial R_2$. First note that, if there is no impurity in the $5 \times 5 \times 3$ supercell, all the Ga and N atoms are equivalent, respectively. Thus only 6 displacements are needed to get all the $\partial^2 E_{\text{bulk}}/\partial R_1 \partial R_2$. We found that even when there is an impurity, when both R_1 and R_2 are away from the impurity (beyond a cutoff distance R_c), the $\partial^2 E/\partial R_1 \partial R_2$ can be approximated by $\partial^2 E_{\text{bulk}}/\partial R_1 \partial R_2$. This good agreement is shown in Fig. S3 of the Supplemental Material [35]. As a result of this approximation, there are only 8 atoms R_2 within a R_c ($= 6.0$ a.u) radius surrounding the impurity, which need explicit numerical displacements to calculate their $\partial^2 E/\partial R_1 \partial R_2$. The accuracy of the final "combined dynamic matrix" (CDM) is further enhanced by enforcing the symmetry condition $\partial^2 E/\partial R_1 \partial R_2 = \partial^2 E/\partial R_2 \partial R_1$, and the sum rule $\sum_{R_1} \partial^2 E/\partial R_1 \partial R_2 = 0$.

The calculated phonon DOSs are shown in Fig. 3. The bulk phonon DOS agrees well with other published phonon spectra [36–38]. For the 71-atom cell, we have compared the CDM method with the explicit full calculation. We see that the CDM describes well the change from bulk DOS to the impurity case DOS. From the 299-atom results, we see that there are some localized phonon peaks near the lower edge of the optical phonon DOS.

Having obtained $\mu_k(R)$ and ω_k, let's now turn our attention to the calculation of electron-phonon coupling constant $F_{s,l}(R) = \langle \psi_s | (\partial H/\partial R) | \psi_l \rangle$. In our case, l is the VBM state, while s is the impurity state as shown in Fig. 2. For a plane wave pseudopotential calculation, there are two contributions to $\partial H/\partial R$, where $H = -\frac{1}{2}\nabla^2 + V_{\text{tot}} + \sum_{l,R} |\phi_{l,R}\rangle\langle\phi_{l,R}|$. The first one comes from the nonlocal pseudopotential operator $\sum_{l,R} |\phi_{l,R}(r - R)\rangle\langle\phi_{l,R}(r - R)|$, with l being the angular momentum, which does not depend on the self-consistent calculation, and hence can be calculated quickly (much like in the atomic force calculations). The second contribution comes from $\partial V_{\text{tot}}(r, R)/\partial R$, where $V_{\text{tot}}(r, R)$ is the self-consistent LDA (or GGA) total potential for a given atomic configuration $\{R\}$. If this is going to

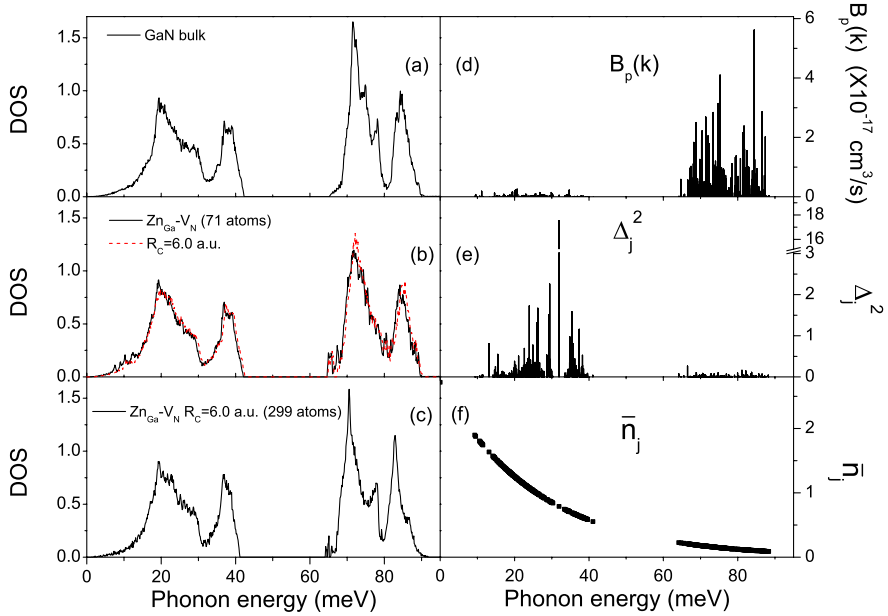

FIG. 3 (color online). The phonon spectrum, (a) for GaN bulk, (b) for $Zn_{Ga}V_N^+$ in 71 atoms, the black solid line is calculated by using all of the atom explicit displacement and the red dashed line is calculated by using the CDM with $R_c = 6.0$ a.u., (c) for $Zn_{Ga}V_N^+$ in 299 atoms and using the CDM with $R_c = 6.0$ a.u. (d) The $B_p(k)$ is the contribution to B_p from different promoting phonon modes k. (e) The contribution to Δ_j^2 from different accepting phonon modes. (f) The contribution to $\bar{n}_j$ from different phonon modes. For (d) and (f), $T = 300$ K.

be calculated directly using numerical displacements, each atomic displacement will need to have a SCF calculation. Then in total $299 \times 3 = 897$ SCF calculations will be needed. However, we will introduce a new algorithm to calculate all these electron-phonon coupling constants at once.

We first define the second contribution (for the $V_{\rm tot}$ term) as

$$F_{sl}^{L}(R) = \int \mathrm{Re}[\psi_s^*(r)\psi_l(r)][dV_{\rm tot}(r)/dR]dr. \quad (5)$$

Let us define $\rho_{sl}(r) = \mathrm{Re}[\psi_s^*(r)\psi_l(r)]$ as a fixed charge density. Then, we can define

$$\rho_\lambda(r) = \sum_{i\epsilon \mathrm{VB}} \psi_i^2(r) + \lambda\rho_{sl}(r) \quad (6)$$

and use $\rho_\lambda(r)$ in the expression of the LDA potential energy U (containing electron-ion, Coulomb, and exchange-correlation energies), so we have

$$E[\psi, R, \lambda] = -\frac{1}{2}\sum_i \langle\psi_i|\nabla^2|\psi_i\rangle + \sum_{i,l,R}\langle\psi_i|\phi_{l,R}\rangle\langle\phi_{l,R}|\psi_i\rangle + U[\rho_\lambda, R]. \quad (7)$$

Here ψ_i are Kohn-Sham orbitals. Now, we can variationally change ψ_i to minimize total energy E, while keeping $\rho_{sl}(r)$ fixed. The SCF calculation is essentially the same as in any given electronic structure codes (we have used our PEtot [39] for this calculation). We then have $\partial E/\partial\psi_i = \epsilon_i\psi_i$, hence $\langle\partial E/\partial\psi_i|\partial\psi_i/\partial X\rangle = 0$ (here X can be R or λ). Let's use F_R to denote the atomic force on atom R, then we have

$$\begin{aligned}\frac{d}{d\lambda}F_R &= \frac{d}{d\lambda}\frac{d}{dR}E[\psi, R, \lambda] = \frac{d}{dR}\frac{d}{d\lambda}E[\psi, R, \lambda] \\ &= \frac{d}{dR}\left\{\sum_i\left\langle\frac{\partial E}{\partial\psi_i}\middle|\frac{\partial\psi_i}{\partial\lambda}\right\rangle + \frac{\partial}{\partial\lambda}E\right\} \\ &= \frac{d}{dR}\left\{\frac{\partial}{\partial\rho_\lambda}U[\rho_\lambda, R]\frac{\partial}{\partial\lambda}\rho_\lambda\right\} \\ &= \int\frac{d}{dR}\{V_{\rm tot}(r, R)\rho_{sl}(r)\}dr \\ &= \int\rho_{sl}(r)[dV_{\rm tot}(r)/dR]dr = F_{sl}^{L}(R). \end{aligned} \quad (8)$$

Note the atomic force F_R can be calculated for all atoms at once, using Hellman-Feynman theory as in conventionally SCF DFT calculations:

$$F_R = \int\rho_\lambda(r)[dV_{\rm ion}(r)/dR]dr + \sum_{i,l,R}2\mathrm{Re}\left\{\left\langle\psi_i|\frac{d}{dR}\phi_{l,R}\right\rangle\langle\phi_{l,R}|\psi_i\rangle\right\}. \quad (9)$$

Thus, following the above procedure, with two SCF calculations (one $\lambda = 0$ and another $\lambda =$ small), we can get all the electron-phonon coupling constants $F_{sl}^{L}(R)$. Such calculated $F_{sl}^{L}(R)$ has been compared with the directly calculated value with numerically obtained $dV_{\rm tot}(r, R)/dR$ (from two R values) in Eq. (5), the results are exactly the same within the numerical accuracy.

With the above calculated C_{sl}^{k}, we can now use Eq. (2) to calculate the nonradiative transition rate. In an actual device, all the hole states should have a finite k point very close to Γ point. With room temperature, the corresponding k is about 0.05 Å^{-1}. As a result the phase factor $\exp(ikr)$ within the localization range of the impurity state $\psi_{\rm im}$ is always close to one (within a 10% error). Thus, we can always use $\psi_{\rm VBM}$ to represent the hole state ψ_l, and $\psi_{\rm im}$ is the final state ψ_s.

W_{sl} from Eq. (2) is the transition rate for the VBM state to the impurity state, which is often written as B_pN_t for a bulk system [3], here N_t is the impurity density and B_p is a capture rate constant. In our case, $N_t = 1/V$ (V is the volume of the supercell), hence $B_p = W_{sl}\cdot V$. Note, in our calculation, W_{sl} will inversely scale with the supercell size, but B_p does not. The results of B_p from a 71-atom cell and 299-atom cell are shown in Fig. S4(a) in the Supplemental Material [35]. They differ by a factor of 1.5. This means the 71 atom cell is not converged, thus the use of a 299-atom cell is necessary.

According to Eq. (2), we can analyze the contribution to the capture rate constant from different promoting phonon modes. This is shown in Fig. 3(d) for room temperature. We see that, most of the contribution comes from the optical phonon modes. On the other hand, the total contribution of the localized phonon mode is relatively small. We also plot Δ_j^2 in Fig. 3(e), which represents the energy stored in each mode in the unit of phonon energy due to the atomic position changes after the electron transition. The D describes the accepting mode coupling strength in the system, with $\bar{n}_j$ shown in Fig. 3(f). We thus see that while the promoting modes come mostly from the optical modes [Fig. 3(d)], the energy conserving accepting modes come mostly from the acoustic modes [Fig. 3(e)]. The existence of these acoustic modes in a solid system also makes the $D\hbar$ relatively large (296 meV in our case) compared with a molecule system [15].

We have studied the transition rate dependence on the impurity energy and temperature. If we fix everything else in Eq. (2), while only change the transition energy ΔE_{sl}, we will have a sensitive dependence on ΔE_{sl} as shown in Fig. 4 especially for low temperature. We have also plotted the transition rate dependence on the temperature in Fig. 4. For small ΔE_{sl}, the temperature dependence is small. For large ΔE_{sl}, B_p increases with T as $\exp(-\Delta E_{sl}/\mathrm{kT})$ when $T > 100$ K. This is due to the excitation of acoustic phonons for $T > 100$ K, and their roles as the accepting modes. B_p are constants when $T < 100$ K. In that temperature regime, most transitions come from phonon mode self-emission. Using our calculated ΔE_{sl} of 0.91 eV, we have $B_p = 5.57 \times 10^{-10}$ cm^3/s at room temperature, and this is near the low end of the experimentally measured range of B_p, which varies from 3×10^{-10} to 3×10^{-6} cm^3/s [5,9].

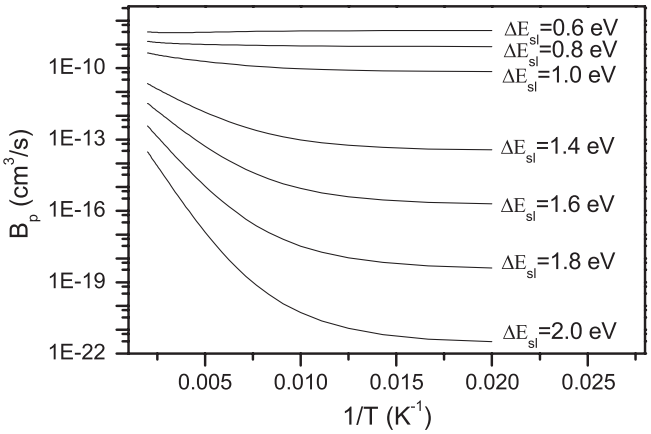

FIG. 4. The function of the nonradiative rate with 1/T for $Zn_{Ga}V_N^+$ in the 299-atom cell.

Our calculated B_p can be used in the SRH formula, where the total hole capture rate is $U_{pc} = B_p p N_t f_t$ [3], where p is hole density, N_t is trap density, and f_t is the probability that the trap is occupied by electron, which is close to 1 in our case.

L.-W. W. was supported by the Director, Office of Science (SC), Basic Energy Science (BES)/Materials Science and Engineering Division (MSED) of the U.S. Department of Energy (DOE) under Contract No. DE-AC02-05CH11231. L. S. was supported by the National High Technology Research and Development Program of China (863 Program) (No. 2011AA03A103), International Cooperation Projects of Ministry of Science and Technology of China (No. 2011DFR50390), and Chinese Academy of Sciences (CAS) overseas study and training program. This research used resources of the National Energy Research Scientific Computing Center.

*lwwang@lbl.gov

[1] W. Shockley and W. T. Read, Phys. Rev. **87**, 835 (1952).
[2] R. N. Hall, Phys. Rev. **87**, 387 (1952).
[3] J. Nelson, *The Physics of Solar Cells* (Imperial College, London, 2003).
[4] T. Tsuchiya, Appl. Phys. Express **4**, 094104 (2011).
[5] M. A. Reshchikov, A. A. Kvasov, M. F. Bishop, T. McMullen, A. Usikov, V. Soukhoveev, and V. A. Dmitriev, Phys. Rev. B **84**, 075212 (2011).
[6] M. A. Reshchikov, A. G. Willyard, A. Behrends, A. Bakin, and A. Waag, Appl. Phys. Lett. **99**, 171110 (2011).
[7] M. A. Reshchikov and H. Morkoc, J. Appl. Phys. **97**, 061301 (2005).
[8] M. A. Reshchikov and R. Y. Korotkov, Phys. Rev. B **64**, 115205 (2001).
[9] S. Jursenas, S. Miasojedovas, G. Kurilcik, A. Zukauskas, and P. R. Hageman, Appl. Phys. Lett. **83**, 66 (2003).
[10] K. Huang and A. Rhys, Proc. R. Soc. A **204**, 406 (1950).
[11] S. H. Lin, J. Chem. Phys. **44**, 3759 (1966).
[12] K. F. Freed and J. Jortner, J. Chem. Phys. **50**, 2916 (1969).
[13] K. F. Freed and J. Jortner, J. Chem. Phys. **52**, 6272 (1970).
[14] C. Deng, Y. Niu, Q. Peng, A. Qin, Z. G. Shuai, and B. Z. Tang, J. Chem. Phys. **135**, 014304 (2011).
[15] Z. G. Shuai, L. Wang, and Q. Li, Adv. Mater. **23**, 1145 (2011).
[16] M. Hayashi, A. M. Mebel, K. K. Liang, and S. H. Lin, J. Chem. Phys. **108**, 2044 (1998).
[17] F. Hetsch, X. Q. Xu, H. K. Wang, S. V. Kershaw, and A. L. Rogach, J. Phys. Chem. Lett. **2**, 1879 (2011).
[18] P. V. Kamat, J. Phys. Chem. Lett. **3**, 663 (2012).
[19] S. Nakamura, Science **281**, 956 (1998).
[20] F. A. Ponce and D. P. Bour, Nature (London) **386**, 351 (1997).
[21] J. Li, S. H. Wei, S. S. Li, and J. B. Xia, Phys. Rev. B **74**, 081201 (2006).
[22] S. Sanna, W. G. Schmidt, T. Frauenheim, and U. Gerstmann, Phys. Rev. B **80**, 104120 (2009).
[23] N. A. Spaldin, Phys. Rev. B **69**, 125201 (2004).
[24] C. G. Van de Walle and J. Neugebauer, J. Appl. Phys. **95**, 3851 (2004).
[25] J. Heyd, G. E. Scuseria, and M. Ernzerhof, J. Chem. Phys. **118**, 8207 (2003).
[26] J. Heyd, G. E. Scuseria, and M. Ernzerhof, J. Chem. Phys. **124**, 219906 (2006).
[27] H. Schulz and K. H. Thiemann, Solid State Commun. **23**, 815 (1977).
[28] G. Kresse and J. Hafner, Phys. Rev. B **47**, 558 (1993); **49**, 14251 (1994); G. Kresse and J. Furthmuller, Phys. Rev. B **54**, 11169 (1996).
[29] S.-H. Wei, Comput. Mater. Sci. **30**, 337 (2004).
[30] Q. M. Yan, A. Janotti, M. Scheffler, and C. G. Van de Walle, Appl. Phys. Lett. **100**, 142110 (2012).
[31] M. Lax, J. Chem. Phys. **20**, 1752 (1952).
[32] V. A. Kovarskii, Fiz. Tverd. Tela (Leningrad) **4**, 1636 (1962) [Sov. Phys. Solid State **4**, 1200 (1962)].
[33] R. Pässler, Czechoslovak Journal of Physics, Section B **24**, 322 (1974).
[34] K. Huang, Scientia Sinica **24**, 27 (1981).
[35] See Supplemental Material http://link.aps.org/supplemental/10.1103/PhysRevLett.109.245501 for relevant derivations for Eqs. (2) and (3), the contribution to $|C_{sl}^k|^2$ from different phonon modes, the forces of all R_2 atoms outside $R_c = 6.0$ a.u., the function of nonradiative rate with temperature, and the function of nonradiative rate with ΔE_{sl} for $Zn_{Ga}V_N^+$.
[36] C. Bungaro, K. Rapcewicz, and J. Bernholc, Phys. Rev. B **61**, 6720 (2000).
[37] K. Parlinski and Y. Kawazoe, Phys. Rev. B **60**, 15511 (1999).
[38] V. Y. Davydov, Y. E. Kitaev, I. N. Goncharuk, A. N. Smirnov, J. Graul, O. Semchinova, D. Uffmann, M. B. Smirnov, A. P. Mirgorodsky, and R. A. Evarestov, Phys. Rev. B **58**, 12899 (1998).
[39] L. W. Wang, "PEtot's Homepage," https://hpcrd.lbl.gov/~linwang/PEtot/PEtot.html.